Reactive transport of micropollutants in laboratory aquifers undergoing transient exposure periods

Maria Prieto-Espinoza, Raphaël Di Chiara Roupert, Benjamin Belfort, Sylvain Weill, Gwenaël Imfeld

Reactive transport of micropollutants in laboratory aquifers undergoing transient exposure periods

Maria Prieto-Espinoza[1,+], Raphaël Di Chiara[1], Benjamin Belfort[1], Sylvain Weill[1], Gwenaël Imfeld[1,*]

[1] Université de Strasbourg, CNRS/EOST, ITES UMR 7063, Institut Terre et Environnement de Strasbourg, Strasbourg, France

*Corresponding author:

Email address: imfeld@unistra.fr (G. Imfeld)

Manuscript for Science of the Total Environment

[+]Present address:

Aix-Marseille Université, CNRS UMR 7376, Laboratoire Chimie Environnement, Marseille, France

Highlights

- Biotransformation of micropollutants in lateral stream-groundwater transition zones
- CSIA data and TPs evidenced caffeine degradation during transient exposure periods
- Model simulations highlight concentration dependency for caffeine biotransformation
- Adaptation of bacterial communities after acute and chronic exposure over 140 days
- Integrative approach for assessing micropollutant biotransformation during stream-groundwater interactions

Graphical abstract

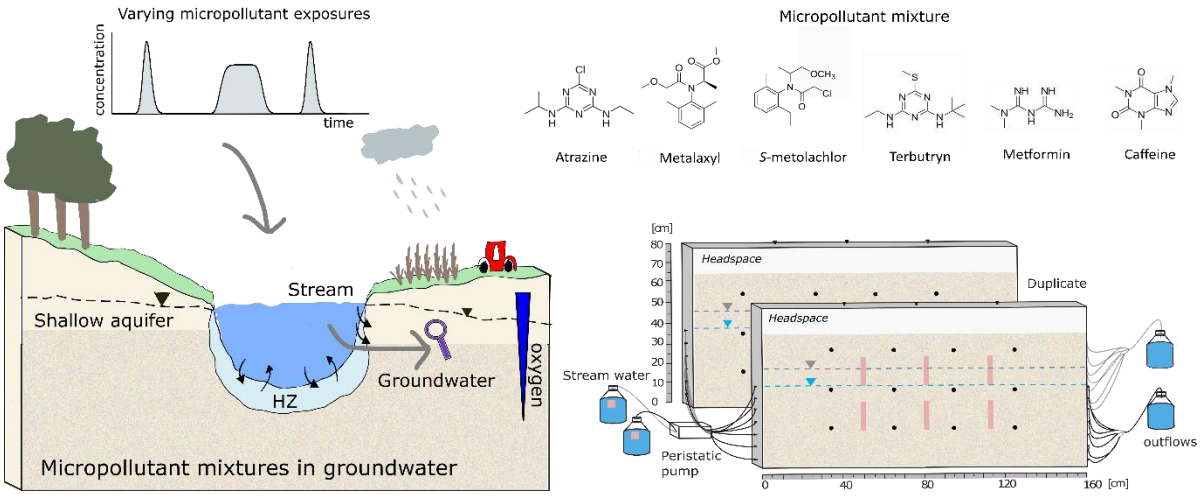

Abstract

Groundwater quality is of increasing concern due to the ubiquitous occurrence of micropollutant mixtures. Stream-groundwater interactions near agricultural and urban areas represent an important entry pathway of micropollutants into shallow aquifers. Here, we evaluated the biotransformation of a micropollutant mixture (i.e., caffeine, metformin, atrazine, terbutryn, *S*-metolachlor and metalaxyl) during lateral stream water flow to adjacent groundwater. We used an integrative approach combining concentrations and transformation products (TPs) of the micropollutants, compound-specific isotope analysis ($\delta^{13}C$ and $\delta^{15}N$), sequencing of 16S rRNA gene amplicons and reactive transport modeling. Duplicate laboratory aquifers (160 cm × 80 cm × 7 cm) were fed with stream water and subjected over 140 d to three successive periods of micropollutant exposures as pulse-like (6000 µg L^{-1}) and constant (600 µg L^{-1}) injections under steady-state conditions. Atrazine, terbutryn, *S*-metolachlor and metalaxyl persisted in both aquifers during all periods (<10% attenuation). Metformin attenuation (up to 14%) was only observed from 90 d onwards, suggesting enhanced degradation over time. In contrast, caffeine dissipated during all injection periods (>90%), agreeing with fast degradation rates ($t_{1/2}$<3 d) in parallel microcosm experiments and detection of TPs (theobromine and xanthine). Significant stable carbon isotope fractionation ($\Delta\delta^{13}C \geq 6.6$ ‰) was observed for caffeine in both aquifers, whereas no enrichment in ^{15}N occurred. A concentration dependence of caffeine biotransformation in the aquifers was further suggested by model simulations following Michaelis-Menten kinetics. Changes in bacterial community composition reflected long-term bacterial adaptation to micropollutant exposures. Altogether, the use of an integrative approach can help to understand the interplay of subsurface hydrochemistry, bacterial adaptations and micropollutants biotransformation during stream-groundwater interactions.

Keywords: micropollutants, biodegradation, CSIA, stream-groundwater interactions, bacterial diversity, modeling

1. Introduction

The ubiquitous release of micropollutants in the environment, typically in the ng L^{-1} to µg L^{-1} range, may result in the deterioration of water quality, aquatic life and human health (Barbosa et al., 2016; Schwarzenbach et al., 2010). Micropollutants cover a wide variety of substances, including pesticides, pharmaceuticals and consumer products. Pesticides are extensively used in agriculture to prevent and control harmful pests and crop yield losses worldwide (Damalas & Koutroubas, 2016). Pharmaceuticals and consumer products, however, are ubiquitously released into aquatic ecosystems, often from inefficient wastewater treatment facilities (Richardson & Kimura, 2016). The frequent and continuous release of micropollutants and their transformation products (TPs) results in their simultaneous presence as complex mixtures in surface water (Bradley et al., 2021; Bradley et al., 2016; Hildebrandt et al., 2008) and groundwater (aus der Beek et al., 2016; Baran et al., 2021; Loos et al., 2010; Masoner et al., 2019; Seiler et al., 1999). However, the transformation of micropollutants in mixtures and their effects on non-target microorganisms in shallow aquifers are still poorly understood.

Natural attenuation in shallow aquifers relies on the ability of microorganisms to break down contaminants into less toxic chemicals (National Research Council, 2000). Micropollutants attenuation results from various biotic and abiotic transformation processes involving biological and chemical reactions, as well as non-degrading processes such as sorption or dilution (Fenner et al., 2013). Biodegradation mainly contributes to the overall contaminant removal in aquifers (Fenner et al., 2013; Meckenstock et al., 2015). However, current concentration measurements are generally not sufficient to infer the contribution of biodegradation to the overall micropollutant removal due to the simultaneous occurrence of both degradative and non-degradative processes. In this context, compound-specific isotope analysis (CSIA) may be used

to evaluate micropollutant degradation by measuring changes of isotope ratios (e.g., $^{13}C/^{12}C$ or $^{15}N/^{14}N$) in the remaining non-degraded molecules. Changes of isotope ratios are related to kinetic isotope effects favoring the cleavage of molecules containing light isotopes compared to heavy isotopes. This results in an isotope fractionation effect in which the remaining contaminant is enriched in heavy isotopes (Elsner, 2010). The resulting change in isotope ratios may be related to micropollutants degradation extent, mechanisms and pathways, although micropollutant CSIA is still an emerging field (Elsner and Imfeld, 2016) in comparison with other industrial pollutants (Ojeda et al., 2019).

In shallow aquifers, the hyporheic zone (HZ), i.e., the transition zone between surface water and groundwater, is located beneath the stream bed and the two sides of the riparian zone (Zhang et al., 2017). The HZ represents a natural biogeochemical barrier against groundwater contamination (Boulton et al., 2010; Lewandowski et al., 2011). However, knowledge on the interplay of dynamic hydrological and biogeochemical conditions with respect to pollutant transformation in the HZ is currently limited. Recently, it has been suggested that HZs sustain micropollutants biotransformation, particularly at the sediment-water interface (SWI) beneath the stream bed (Droz et al., 2021; Mechelke et al., 2020; Peter et al., 2019; Schaper et al., 2018). The reactivity of this zone is driven primarily by hydraulic residence times, surface-groundwater exchange, mass transfer rates, nutrient turnover and bacterial diversity (Conant et al., 2019; Drouin et al., 2021; Peter et al., 2019; Posselt et al., 2020). Because oxygen gradients are established across the HZ, anoxic conditions are usually observed at the bottom of the SWI. This may lower micropollutants degradation rates (Droz et al., 2021), and thus increase their potential mobilization and accumulation in shallow groundwater (Hintze et al., 2020; Iker et al., 2010; Jakobsen et al., 2019; Lesser et al., 2018; Loos et al., 2010). In conditions where the stream level

is higher than the adjacent groundwater, e.g., due to seasonal hydrological changes (Winter et al., 1998), the losing streams may laterally flow into groundwater (Ghysels et al., 2021; Winter et al., 1998), and further mobilize micropollutants into oxygen-rich zones in shallow aquifers (Chen & Chen, 2003; Derx et al., 2010; Hancock, 2002). This lateral transition zone represents a yet poorly understood mixing zone of stream-groundwater biogeochemical dynamics. In addition, shallow aquifers in connection to streams are subjected to seasonal variations of micropollutants inputs, resulting in acute and chronic exposure periods possibly affecting micropollutants biotransformation.

Laboratory aquifers have proven advantageous to study the main drivers of micropollutants biotransformation under controlled conditions, while considering the spatial and temporal gradients formed across porous media (Bauer et al., 2009; Prieto-Espinoza et al., 2021; Schürner et al., 2016; Sun et al., 2021a; Ye et al., 2015). Recently, the use of CSIA in laboratory aquifers has shed light on micropollutant biotransformation, emphasizing the role of sorption and degradation kinetics (Schürner et al., 2016), diffusion and transverse-dispersion (Sun et al., 2021b), and mass-transfer limitations (Sun et al., 2021a). However, an integrative understanding of the attenuation of micropollutant mixtures and the long-term change of groundwater bacterial diversity in response to environmental perturbations at the lateral stream-groundwater interface is yet required.

The purpose of this study was thus to examine the reactive transport of a micropollutant mixture in laboratory aquifers continuously fed with stream water mimicking stream-groundwater interactions dominated by lateral stream water flow to adjacent groundwater. The micropollutant mixture was composed of the herbicides atrazine, terbutryn and *S*-metolachlor, the fungicide metalaxyl, the consumer product caffeine, and the anti-diabetic drug metformin.

The selected micropollutants represent different classes of substances with described degradation pathways and TPs, distinct half-lives and which may co-occur in surface water and groundwater (Bradley et al., 2021; Masoner et al., 2019). Duplicate laboratory aquifers underwent a series of consecutive pulse (acute) and constant (chronic) exposure periods (over 140 days). The pulse-like and constant exposure periods represented factors affecting micropollutant trends, such as (acute) hydrological events (e.g., flooding events, surface runoff) (Chow et al., 2020) and (chronic) seasonal applications (Baran et al., 2021). We hypothesized that transient exposures to micropollutants may affect bacterial communities and thus micropollutants degradation in shallow groundwater adjacent to streams. Micropollutants and their TPs concentrations, C− and N−CSIA, and DNA analysis (i.e., 16S rRNA amplicons) were performed to evaluate the biotransformation of the micropollutant mixture. Concentrations and CSIA data were further interpreted using a simple reactive transport model. In addition, parallel biotic and abiotic microcosm experiments with stream water were conducted under oxic conditions to evaluate degradation kinetics of the micropollutants.

2. Materials and methods

2.1 Stream water collection

Stream water was collected from the Souffel sub-catchment (3.6 km^2 out of 120 km^2 of total catchment area) located 30 km northeast of Strasbourg (Bas-Rhin, France; 48°40'09.4"N 7°33'51.5"E). With conventional agriculture accounting for 80% of the land use, of which 12% corresponds to urban areas and 8% forests, the Souffel catchment is categorized as severely impacted by pesticide contamination. Corn and sugar beets are the main crops, receiving pesticide applications as observed in nearby and similar agricultural catchments (Alvarez-

147 Zaldívar et al., 2018; Droz, 2020; Lefrancq et al., 2017). For this study, freshwater was collected
148 every two months from January to September 2020 in three sterile 50 L stainless steel containers,
149 which were stored at 18 ± 1° C until further use. Total organic carbon was 2.84 ± 0.67 mg L^{-1} (*n*
150 = 5) and pH was 7.1 ± 0.2 in the Souffel stream water. Background concentrations of
151 micropollutants were measured at the beginning of the sampling campaign, where only caffeine
152 (4.4 ng L^{-1}) and *S*-metolachlor (43 ng L^{-1}) were detected. For hydrochemical and bacterial
153 diversity analyses, the stream water was collected in sterile 1 L glass bottles, transported on ice
154 and stored immediately at 4 ± 1° C until further analyses.

155 **2.2 Micropollutants**

156 A detailed description of chemical reagents of the micropollutant mixture, corresponding
157 TPs, and their physicochemical properties is provided in the Supporting Information (SI, Section
158 A). The micropollutant mixture consisted of atrazine, caffeine, metalaxyl, *S*-metolachlor and
159 terbutryn purchased from Sigma-Aldrich (St: Louis, MO, USA; analytical grade purity: >99%).
160 A stock solution containing a mixture of these chemicals was prepared in acetonitrile (ACN) at 5
161 g L^{-1} and stored at –20 °C. Metformin was purchased from Sigma-Aldrich (St: Louis, MO, USA;
162 analytical grade purity: >99%) and prepared in water at 5 g L^{-1} and stored at 4 °C. In addition,
163 the following TPs were purchased: desethylatrazine, deisopropylatrazine, hydroxyatrazine,
164 theobromine, paraxanthine, xanthine, carboxylic acid metalaxyl, demethylmetalaxyl, metolachlor
165 ESA, metolachlor OXA, desethylterbutryn, desethyl-2-hydroxy-terbutryn, terbutryn-2-hydroxy,
166 1,3,5-triazine, and guanylurea. Stock solutions of the TPs were prepared in MeOH at 1 g L^{-1} and
167 stored at –20 °C.

168 **2.3 Degradation kinetic experiments**

Biodegradation microcosm experiments were performed to examine micropollutant attenuation in the stream water serving as inflow water of both laboratory aquifers. Biotic and abiotic microcosms were conducted under oxic conditions in a sacrificial mode at room temperature (20 ± 2°C) and in dark at natural pH (7.3 ± 0.4). Microcosms were prepared in 20 mL headspace vials crimped with butyl/PTFE caps (Interchim®) with a total volume of 15 mL of stream water. Micropollutants were spiked to reach the final concentration of 6 mg L^{-1} per compound, representing the maximum concentrations established at the inflow of both laboratory aquifers. High micropollutant concentrations were needed to allow reliable C− and N−CSIA (Droz et al., 2021). The solutions were stirred under sterile conditions until complete ACN evaporation. To maintain oxic conditions (4−9 ppm O_2), limit water loss and avoid microbial contamination, a 0.2 µm PTFE syringe filter (Rotilabo®) was mounted on a syringe tip, which was stuck through the vial cap (Droz et al., 2021). All microcosms were kept under constant shaking (orbital shaker at 120 rpm). Biotic experiments were prepared in triplicates and sacrificed on days 0, 2, 5, 15, 50, 80, 100 and 200. Abiotic experiments (autoclaved triplicate experiments) and blanks were sacrificed on days 0, 5, 50 and 200. A 2 mL aliquot was used for hydrochemical analysis, while a 1 mL aliquot was collected to quantify metformin and TPs. The remaining volume (12 mL) was used for micropollutants quantification and C− and N−CSIA (i.e., $\delta^{13}C$ and $\delta^{15}N$). Metformin CSIA was not performed due to its high polarity and low volatility hampering GC-IRMS measurements.

2.4 Experimental setup and operation of laboratory aquifers

Experiments were conducted in two parallel laboratory aquifers with dimensions of 160 cm × 80 cm × 7 cm (length × height × width) and filled with sterile quartz sand (grain size: 0.4−0.6 mm; depth: 70 cm) (Figure 1). A detailed description of the experimental setup is

provided in the SI (Section B). Both aquifers were setup as duplicate and continuously fed in parallel with stream water at a rate of 1.15 L d^{-1}. The water table was positioned at 43 cm from the bottom. All injection ports from each aquifer were connected to 10 L reservoirs with continuously stirred inflow water (Figure 1). The inflow water remained oxygenated (8.6 mg L^{-1}) and an atmospheric exchange from the top ports of the aquifers maintained oxic conditions throughout the experiments. The outflow reservoirs consisted of sterile 5 L bottles connected to all outflow sampling ports of each aquifer. Results from hydrochemistry, DNA, concentrations and CSIA thus represent depth-integrated water samples (i.e., mixing of all flow paths). The saturated zone (SZ, z = 0–43 cm) was characterized by mean dissolved O_2 concentrations of 4.4 ± 0.8 mg L^{-1}. Experiments were conducted in a temperature-controlled room at 18 ± 1 °C, and both aquifers were protected from light. The injection of a saline conservative tracer (NaCl; 1 L solution at 1 g L^{-1}) prior to the experiments enabled to estimate the average pore water velocity at 0.08 m d^{-1} (SI, Section C).

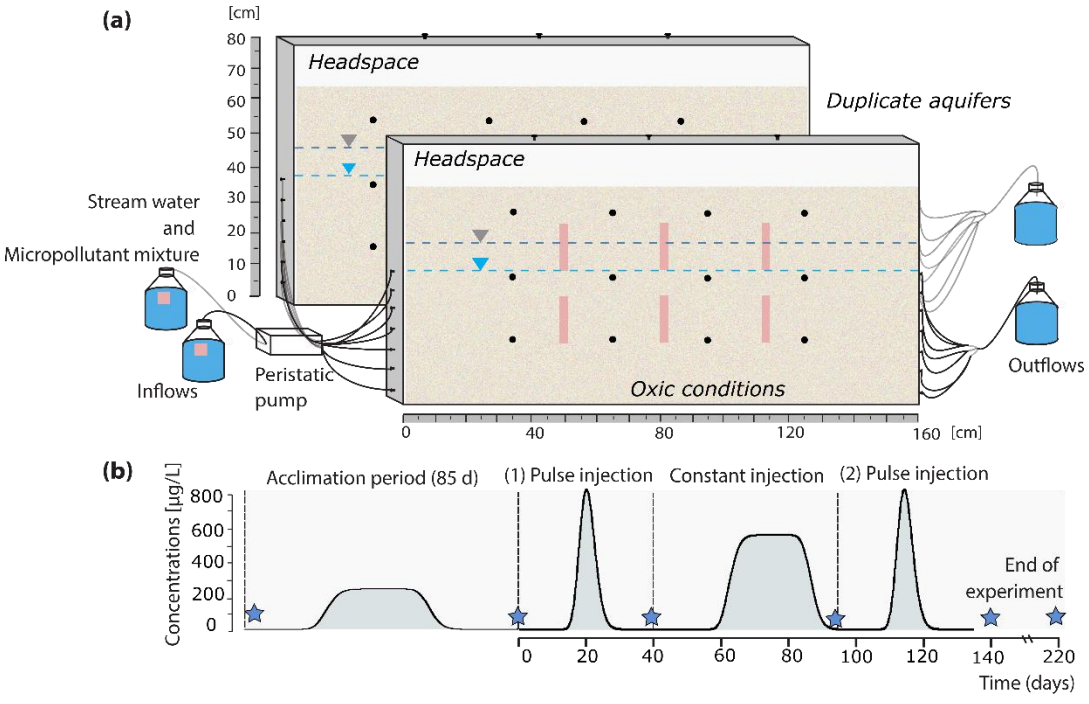

Figure 1. Laboratory aquifers fed with stream water and exposed to a micropollutant mixture. (a) Schematic overview of the laboratory aquifers. Stream-groundwater flows from left to right of the aquifers. Water samples were retrieved from sampling ports (black dots) across the sand compartment, and the outflow reservoirs (depth-integrated outflow bottles). Oxygen concentrations were followed across the porous media (pink rectangles). Upper ports of the aquifers, consisting in 0.2 µm PTFE syringe filter mounted on a Luer-Lock valve, remained open to allow gas exchange with the atmosphere. (b) Aquifer operations, including an acclimation period prior to the experiments, and subsequent periods of pulse and constant injection of micropollutants. Dotted lines represent micropollutant injections and blue stars indicate sampling for bacterial diversity analysis. Breakthrough curves of the micropollutants were monitored at the outflow reservoirs.

After injection of the conservative tracer, the aquifers were fed with stream water for 60 d (i.e., at least two pore water volumes) to ensure complete NaCl removal. An acclimation period was then established by injecting a pulse of the micropollutant mixture (1 L solution at 6 mg L^{-1}) for 85 d to support adaptation of the bacterial community and favor micropollutants biodegradation (Poursat et al., 2019a; Prieto-Espinoza et al., 2021; Sun et al., 2021a). No samples were collected during the acclimation period. For the experiment, three consecutive injection periods were performed in each aquifer over 140 d (Figure 1), mimicking acute and chronic micropollutants inputs driven by seasonal applications and hydrological events (Baran et al., 2021; Chow et al., 2020). At the beginning of the experiment (i.e., day 0; Figure 1), a first pulse injection of the micropollutant mixture (1 L at 6 mg L^{-1} for each micropollutant) was conducted. From days 40 to 61, the micropollutant mixture at 10 times lower concentrations (600 µg L^{-1}) was constantly injected. Finally, a second pulse injection (1 L at 6 mg L^{-1}) was performed at day 93. Unspiked stream water fed the aquifers after each injection period (Figure 1), and from 140 to 220 d to flush out micropollutants prior to collection of core sand samples. To limit

233 micropollutants degradation in the inflow reservoirs during the constant injection phase, the
234 inflow reservoirs were replaced daily by freshly prepared spiked solutions.

2.5 Sampling procedure

For micropollutant concentration analysis, TPs and CSIA (i.e., $\delta^{13}C$ and $\delta^{15}N$), 1 L water samples were collected from the outflow reservoirs (Figure 1), immediately filtered on 0.45 µm NC membranes and stored at 4 °C until further analysis. Sampling resolution during the pulse and constant injection periods was approximately every 24 h and 48 h, respectively. For TPs analysis, a 1 mL water aliquot was used. Only samples from the second pulse injection (90-140 d) were screened due to evidence of several micropollutants degradation only after 90 d (see below). For hydrochemical analysis, a 30 mL aliquot was collected every 5 d from the inflow and outflow reservoirs. For DNA extraction, 200 mL were also collected from the inflow and outflow reservoirs at the beginning of the acclimation period, and during the experimental period at 0, 38, 90, 140 and 220 d (Figure 1). In addition, two depth-integrated pore water samples (10 mL) were collected from each aquifer at 45 cm and 105 cm from the inflows prior to the acclimation period, and at 38, 140 and 220 d. Water samples were filtered through sterile 0.22 µm membrane filters (Swinnex holder, 13 mm, Millipore, Bedford, USA) and stored at –20 °C until DNA extraction. At the end of the experiments (220 d), four integrative sand cores were retrieved from each aquifer for DNA analysis at 45 cm and 105 cm from the inflow, and at depths of 15 cm and 45 cm. Each subsample core was thoroughly mixed. A subsample of 1 g of sand was used for DNA extraction.

2.6 Analytical methods

2.6.1 Hydrochemistry

Oxygen (O_2) concentrations were monitored *in situ* by O_2 sensitive optode foils (PreSens GmbH, Regensburg, Germany) located at the inlet reservoirs and across the aquifers (Figure 1). Redox potential (Eh), pH and electrical conductivity were monitored using laboratory probes

(SCHOTT® Instruments). Major ions were measured by ion chromatography (Dionex ICS-5000, Thermo Scientific, USA). Total organic carbon (TOC), dissolved organic carbon (DOC) and dissolved inorganic carbon (DIC) were analyzed by a TOC analyzer (TOC−V−CPH Shimadzu, NF EN 1484).

2.6.2 Micropollutants extraction and quantification

Solid phase extraction (SPE) of pesticides and caffeine was carried out using SolEx C18 cartridges (1 g, Dionex®, CA, USA) and an AutroTrace 280 SPE system (Dionex®, CA, USA), following an in-house method described previously (Droz et al., 2021; Elsayed et al., 2014). A detailed description of micropollutants extraction and quantification methods is provided in the SI (Section D). All pesticides and caffeine were quantified by gas chromatography (GC, Trace 1300, Thermo Fisher Scientific) coupled with a mass spectrometer (MS, ISQ™, Thermo Scientific). Metformin was quantified by liquid chromatography (UHPLC, Ultimate 3000, Thermo Fisher Scientific) coupled with a tandem mass spectrometer (MS/MS, TSQ Quantiva, Thermo Fisher Scientific).

2.6.3 Compound-specific isotope analysis (CSIA)

A detailed description of the analytical methods is provided in the SI (Section E). Stable carbon and nitrogen isotope composition of pesticides and caffeine were determined by gas chromatography−combustion−isotope ratio mass spectrometry (GC−C−IRMS), with a gas chromatograph (Trace 1310) coupled via a GC/Conflow IV interface to an isotope ratio mass spectrometer (Delta V plus, Thermo Fisher Scientific). In-house standards were prepared daily and analyzed prior to sample measurements. Carbon and nitrogen isotope ratios were reported in δ notation as parts per thousand (‰) relative to the international reference material Vienna Pee Dee-Belemnite (V-PDB) (Coplen et al., 2006) and air standards, respectively. The total

analytical uncertainty (1σ) of measurements was ≤0.5‰ for $\delta^{13}C$ and ≤1 ‰ for $\delta^{15}N$ values, within the linearity range (6−300 ng for C and 40−300 ng for N) (Droz et al., 2021). The average isotope value of the residual non-degraded fraction of the micropollutants was derived according to the Rayleigh equation (Elsner, 2010):

$$ln\left(\frac{R_{t,E}}{R_{0,E}}\right) = ln\left(\frac{C_{t,E}}{C_{0,E}}\right) \cdot \varepsilon_{bulk}^{E} \quad (1)$$

where $R_{t,E}/R_{o,E}$ is the isotope ratio of element "E" (i.e., $^{13}C/^{12}C$ and $^{15}N/^{14}N$), and $C_{t,E}$ and $C_{0,E}$ are the concentrations at a given time (t) and at the initial time (0), respectively. Carbon and nitrogen isotopic composition were reported in delta notation ($\delta^{h}E$) following $\delta^{h}E = [(R_{sample}/R_{standard}) - 1] \times 1000$ (Elsner, 2010). Apparent isotope fractionation values (ε_{bulk}^{E}, in ‰) were obtained by least-squares linear regression without forcing the slope through the origin. The uncertainty corresponds to the 95% confidence interval and the error was determined using ordinary linear regression (Elsner et al., 2007).

2.7 DNA extraction and sequencing

For both pore water and sand core samples, DNA was extracted using the DNeasy Power Water kit according to the manufacturer's protocol (Qiagen, Hilden, Germany). Extracted DNA was quantified using Qubit fluorometric quantification with the Qubit dsDNA HS Assay kit (Thermo Fischer Scientific, MA, USA). A detailed description of DNA sequencing is given in the SI (Section F). Sequencing data from pore water and sand samples were deposited to the ENA archive, BioProject accession number PRJEB52684. Multivariate statistical analysis of relative observed taxonomical units (OTU) abundance was performed with R (Hellal et al., 2021). Non-metric multidimensional scaling (NMDS) based on Bray-Curtis dissimilarities of log-transformed data was performed to visualize dissimilarities between bacterial taxa (Hellal et al., 2021). Analysis of similarities (ANOSIM, *n*=31 samples) was used to infer statistical

differences between groups of community profiles (Torabi et al., 2020). Datasets obtained from Illumina sequencing were also used to compute α-diversity indices and for rarefaction analysis (SI, Section F). In total, 1,861,511 high-quality sequences were obtained (n=31 for pore water and n=8 for sand samples). Rarefaction curves of diversity indices reached asymptotes with increasing sequencing depth, indicating sufficient sequencing efforts to capture the biodiversity extent of bacterial communities in all samples (SI, Section F).

2.8 Reactive transport modeling

Carbon isotope fractionation was only considered for the model description because significant nitrogen isotope fractionation was not observed in this study (see Section 3.3). The model was simplified to a one-dimensional domain in accordance with the experimental setup mirroring transient exposure periods in a shallow aquifer (Figure 1). Oxygen transport was not considered due to a lack of temporal high-resolution oxygen data. The simple reactive transport model considering equilibrium sorption was described as (Eckert et al., 2013):

$$^{12}R\frac{\partial c^{12}}{\partial t} + v\frac{\partial c^{12}}{\partial x} = D\frac{\partial^2 c^{12}}{\partial x^2} + r_{deg}^{12} \quad (2)$$

$$^{13}R\frac{\partial c^{13}}{\partial t} + v\frac{\partial c^{13}}{\partial x} = D\frac{\partial^2 c^{13}}{\partial x^2} + r_{deg}^{13} \quad (3)$$

Here, $c_{tot}=c^{12}+c^{13}$ (µg L^{-1}) is the total concentration of the two most abundant micropollutant light (^{12}C) and heavy (^{13}C) isotopologues. R (-) is the retardation factor accounting for equilibrium sorption as $R = 1 + \frac{\rho_b}{n}K_d$, in which ρ_b (kg L^{-1}) is the dry bulk density of the sediment, n (-) is the porosity assumed as 0.37 (-), and K_d (L kg^{-1}) is the linear distribution coefficient between water and sediment phases of the isotopologues. v (m s^{-1}) is the average water velocity, and D (m^2 s^{-1}) is the hydrodynamic dispersion value. The degradation rates r_{deg} (µg $L^{-1}s^{-1}$) of the two most abundant light (^{12}C) and heavy (^{13}C) isotopologues,

assuming Michaelis-Menten kinetics (Eckert et al., 2013; Van Breukelen & Prommer, 2008), are given by:

$$r_{deg}^{12} = -r_{max}^{12} \frac{c^{12}}{K_m^{12}\left(1+\frac{c^{12}}{K_m^{12}}+\frac{c^{13}}{K_m^{13}}\right)} \quad (4)$$

$$r_{deg}^{13} = -r_{max}^{13} \frac{c^{13} \cdot \alpha_B}{K_m^{13}\left(1+\frac{c^{12}}{K_m^{12}}+\frac{c^{13}}{K_m^{13}}\right)} \quad (5)$$

where r_{max} is the maximum degradation rate and K_m is the half-saturation concentration (μg L^{-1}) of the light (^{12}C) and heavy (^{13}C) isotopologues. To compute degradation rates of the isotopologues, K_m is assumed to be identical for both isotopologues, as suggested previously (Eckert et al., 2013; Van Breukelen & Prommer, 2008). The isotope fractionation factor α_B (-) is thus defined as:

$$\alpha_B = \frac{r_{deg}^{13}/c^{13}}{r_{deg}^{12}/c^{12}} \quad (6)$$

Isotope fractionation by transverse dispersion was not considered, since insignificant isotope effects by transverse dispersion have previously been shown for micropollutants reactive transport in flow-through laboratory aquifers (Schürner et al., 2016; Sun et al., 2021b). Although sorption is not expected to be significant in our experimental setup (clean quartz sand as the solid matrix), isotope fractionation affected by equilibrium sorption was modeled considering that light isotopes tend to sorb slightly more than heavier isotopes (i.e., $^{12}K_d > {}^{13}K_d$) (Kopinke et al., 2005). Isotope fractionation affected by sorption is thus described as (Schürner et al., 2016):

$$\alpha_{sorp} = \frac{{}^{13}R-1}{{}^{12}R-1} = \frac{{}^{13}K_d}{{}^{12}K_d} \quad (7)$$

The breakthrough curve (BTC) of the conservative tracer was fitted to retrieve the average velocity υ and the longitudinal dispersion coefficient D. To avoid disturbing *endogenous* bacterial communities of the injected stream water during transient micropollutant exposures, a

conservative tracer could not be injected during the experiments. Conservative transport according to transport parameters of the NaCl tracer was thus simulated for all injection periods and compared to the micropollutant BTCs. All model results are presented for the depth-integrated outflow reservoirs (x = 160 cm). The fitted transport parameters, the fitting procedure and a description of the modeled scenarios are provided in the SI (Section G). Briefly, the coupled system of one-dimensional reactive-transport equations is solved in a fully implicit and fully coupled mode using a cell-centered Finite Volume Method combining a Lax-Wendroff 2nd order scheme of the advective term for spatial discretization. All model parameters are assumed to be spatially uniform. Finally, isotope fractionation values associated with micropollutants biotransformation (ε_B, ‰) and sorption (ε_{sorp}, ‰) were calculated as $\varepsilon = (\alpha - 1) \times 1000$.

3. Results and discussion

3.1 Kinetics of micropollutants biotransformation in stream water microcosms

Microcosm experiments confirmed contrasted biotransformation potential of the selected micropollutants in the Souffel stream water. In biotic experiments under oxic conditions, a gradual decrease of nitrate concentrations suggested co-occurrence of nitrate reduction after 50 d (SI, Section H). The hydrochemical conditions did not change significantly under abiotic conditions (SI, Section H). Under abiotic conditions, less than 10% of the initial mass dissipated after 200 d, corresponding to analytical uncertainties. This indicates insignificant abiotic reactions, such as hydrolysis, and that biodegradation prevailed under biotic conditions.

Under biotic conditions, caffeine rapidly dissipated ($t_{1/2}$ = 3 d; Figure 2), agreeing with previous studies showing rapid half-lives of caffeine ($t_{1/2}$ < 4 d) in river water microcosms (Lam et al., 2004; Nödler et al., 2014). Accordingly, caffeine $\delta^{13}C$ values increased from –31.4 ± 0.1‰

up to –26.6 ± 0.2‰ (SI, Section I). The estimated ε_c value of caffeine of –1.1 ± 0.3 ‰ agreed with previous observations in a SWI batch experiment where slight but significant fractionation ($\Delta\delta^{13}C>2‰$) occurred after >90% of caffeine degradation (ε_c = –0.7 ± 0.1 ‰) (Droz, 2020). However, no changes in $\delta^{15}N$ values were observed. Caffeine biodegradation via the *N*-demethylation pathway has been suggested as the most common caffeine biodegradation pathway in at least 80% of the reported isolates characterized worldwide (Summers et al., 2015), with a sequential transformation of caffeine to theobromine to xanthine (Dash & Gummadi, 2007; Yu et al., 2009). The detection of theobromine and xanthine in the biotic stream water microcosms further supported caffeine biodegradation via the *N*-demethylation pathway (SI, Section H).

Contrastingly, *S*-metolachlor dissipated by 20% in the first 5 d, while overall attenuation was up to 60% after 200 d ($t_{1/2}$ = 187 d; Figure 2). This agrees with reported half-lives of *S*-metolachlor ranging from 56 to 182 d in agricultural soils and SWI microcosms (Drouin et al., 2021; Torabi et al., 2020). Metformin and metalaxyl started dissipating after 50 d and 100 d with estimated half-lives of 189 d and 147 d, respectively (Figure 2). Previous studies reported half-lives of metalaxyl ranging from 9 to 127 d in agricultural soils (Buerge et al., 2003), while metformin has been classified as a not readily biodegradable substance with half-lives ranging from 28 to 98 d in activated sludge (Straub et al., 2019). On the other hand, terbutryn and atrazine dissipated to up to 30% and 38% of their initial mass at 200 d, respectively (Figure 2). Half-lives of atrazine and terbutryn, assuming pseudo-first order degradation, were estimated as 225 d and 290 d, respectively, agreeing with observed long half-lives for terbutryn ($t_{1/2}$ = 177–349 d) in groundwater microcosms under oxic conditions (Talja et al., 2008).

Carbon and nitrogen isotope fractionation of atrazine, terbutryn, metalaxyl and *S*-metolachlor were not observed after 200 d, confirming limited biodegradation (SI, Section I). However, TPs formation confirmed that biodegradation was the main attenuation process (SI, Section H). Overall, our results suggest the occurrence of a lag-phase of 50 d before slow biotransformation of metformin, and of 100 d for atrazine, terbutryn, and metalaxyl in stream water microcosms (Figure 2). Such lag-phase has also been observed for atrazine and metolachlor degradation in biotic groundwater microcosms (Cavalier et al., 1991; Schwab et al., 2006), and may be attributed to early stages of bacterial adaptation to chemical exposure (Poursat et al., 2019a), and to the effect of chemical mixtures on bacterial growth (Reardon et al., 2002). However, the degradation kinetics of the selected micropollutants in the stream water microcosms were similar to those previously reported individually and at lower concentration ranges (e.g., Cavalier et al., 1991). Hence, the degradation kinetics in the stream water microcosms may be related to the physicochemical properties of each micropollutant (SI, Section A), where the faster kinetics were observed for the most soluble compounds.

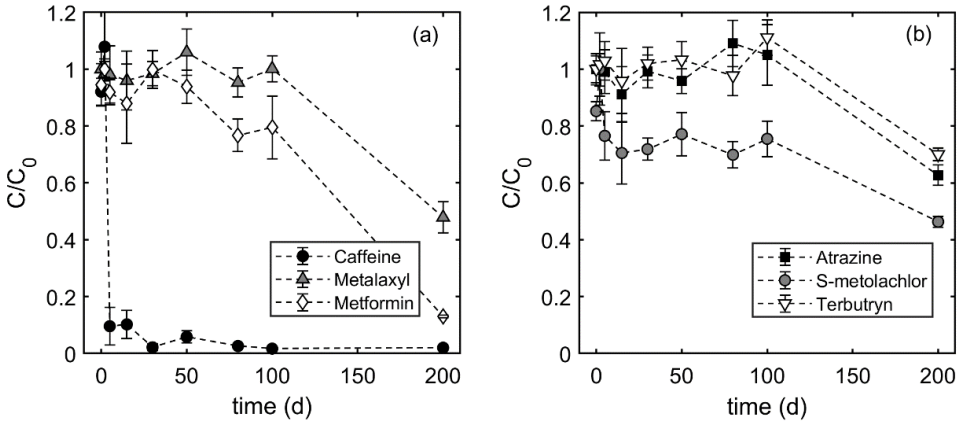

Figure 2. Biodegradation of micropollutants in biotic (oxic) stream water microcosms. (a) Caffeine, metalaxyl and metformin, and (b) atrazine, *S*-metolachlor and terbutryn. Error bars represent the total uncertainty of measurements (n=3).

3.2 Micropollutants biotransformation in flow-through laboratory aquifers

The dynamics of hydrochemical conditions and micropollutant concentrations in both aquifers were similar, supporting the reproducibility of the duplicate laboratory aquifers. At the end of the 85-days acclimation period, background concentrations of micropollutants ranged from 1 to 10 µg L^{-1} at the outflows. Overall, hydrochemical conditions in both aquifers remained constant throughout the experiment (0−140 d) (SI, Section J). Oxic conditions (mean dissolved O_2 concentration: 4.4 ± 0.8 mg L^{-1}) prevailed in both aquifers over time and across the depth of the SZ. However, nitrate concentrations decreased at end of the constant and second pulse injection periods (from 70-90 d and 130-140 d, respectively), while ammonium concentrations increased, suggesting nitrate reduction in the aquifers (SI, Section H). This suggests the formation of sub-anoxic micro-zones near the aquifer outlets, e.g., due to the formation of biomass hot spots or sand clogging, resulting in faster oxygen depletion in these zones. However, oxygen consumption during micropollutants BTCs could not be evidenced due to a lack of temporal high-resolution oxygen data (SI, Section H), while nitrate-reducing bacteria in the aquifers were not observed (SI, Section O).

Mass recoveries of each micropollutant are provided in SI (Section K). *Caffeine* biotransformation in the laboratory aquifers occurred during all examined injection periods (0−140 d), and readily dissipated compared to the other micropollutants (Figure 3, upper panel). This is in agreement with the fast caffeine biodegradation kinetics in the stream water microcosms (Figure 2) and previous lysimeter experiments (Koroša et al., 2020). Caffeine biodegradation was the main attenuation process as abiotic transformation was insignificant in the stream water microcosms (SI, Sections H and I) and sorption is expected to be insignificant due to low organic content (<0.01%) in the quartz sand matrix of the aquifers. Caffeine

biodegradation in the aquifers was also supported by the detection of caffeine TPs, i.e., theobromine (up to 1460 µg L^{-1}) and xanthine (up to 328 µg L^{-1}), during the second injection period with similar retentions times as the parent compound (SI, Section L). These high TP concentrations suggest that further caffeine mineralization did not occur in the aquifers compared to the stream water microcosms (SI, Section H), likely due to shorter retention times. Overall, fast caffeine attenuation may be associated with microorganisms adapted to constant and long periods of caffeine inputs into surface waters (Summers et al., 2015). At least 71 bacterial strains from many different habitats worldwide are involved in caffeine biodegradation, possibly sustained by ancient metabolic pathways for methylxanthines (Summers et al., 2015; Vega et al., 2021).

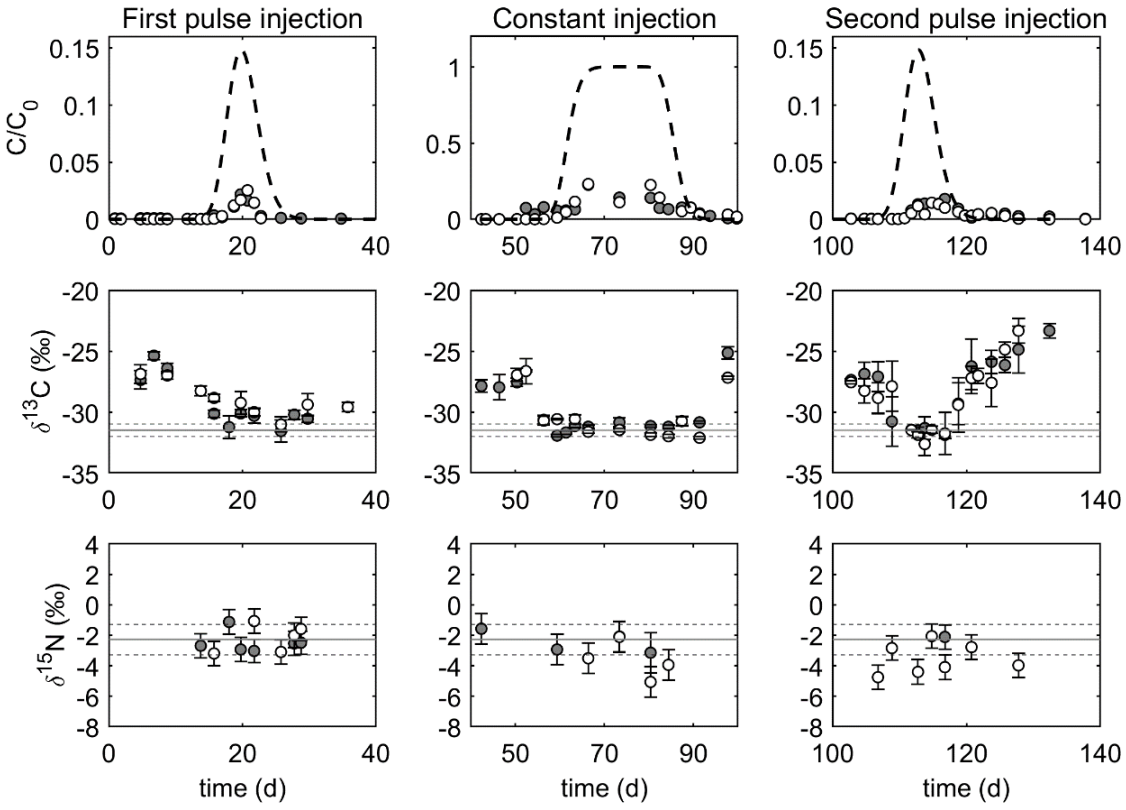

Figure 3. Caffeine concentrations (upper panel) and carbon ($\delta^{13}C$) and nitrogen ($\delta^{15}N$) isotope ratios (middle and lower panels) during the transient exposures of micropollutants. Full and

empty symbols represent data sets from the duplicate aquifers. Dashed back lines represent modeled BTCs of the saline conservative tracer (upper panel). Error bars correspond to the total analytical uncertainty, which incorporates both accuracy and reproducibility of n=3 measurements. Grey horizontal lines (middle and lower panels) indicate the reference isotope signatures of caffeine standards measured by EA−IRMS for $\delta^{13}C$ (−31.40 ± 0.02 ‰) and $\delta^{15}N$ (−2.28 ± 0.06 ‰). Dashed horizontal lines (middle and lower panels) represent the total uncertainty of carbon ±0.5‰ and nitrogen ±1‰ isotope analysis.

Metformin attenuation in the laboratory aquifers increased over time. During the first pulse injection (0–40 d), the BTC of metformin and the conservative tracer were similar (SI, Section K), and no significant metformin attenuation was observed during the constant injection period (40–90 d). In contrast, during the second pulse injection (90–140 d), only 82 ± 5 % of the initial mass of metformin was recovered (SI, Section K). This indicates that metformin biodegradation in the aquifers occurred mostly from 90 to 140 d. Metformin biodegradation is also supported by results of the stream water microcosms (Figure 2) and the detection of its main TP guanylurea in the aquifers (Poursat et al., 2019b) (SI, Section L). Overall, an increase in metformin attenuation over time suggests a gradual adaptation or an increase of active bacterial degraders following the acclimation and subsequent periods (from 0 to 90 d) of metformin exposure. A similar bacterial adaptation has been suggested previously in chemostat systems, where a 2-month pre-exposure period enhanced metformin degradation, correlating with an increase in bacterial community diversity, composition and activity (Dalmijn et al., 2021).

Contrastingly, *S-metolachlor* showed similar BTCs as those of the conservative tracer throughout the whole experiment (SI, Section K), suggesting limited *S*-metolachlor biodegradation in the aquifers. The limited *S*-metolachlor biodegradation mirrored the slow *S*-metolachlor degradation kinetics after 100 days in the stream water microcosms (Figure 2). This contradicts the idea that *S*-metolachlor degraders in the inflow stream water may be already adapted to long periods of *S*-metolachlor applications in the field (Lefrancq et al., 2017). However, a previous study of oxic groundwater microcosms amended with a herbicide mixture (up to 5 µg L^{-1}) consisting of alachlor, metolachlor and propanil showed that metolachlor persisted during the first 12 months, while significant (up to 46 %) biodegradation occurred only after 18 months (Cavalier et al., 1991). Minimal *S*-metolachlor degradation was also observed

478 during the early stage (first 20 y) of a groundwater plume (1−820 µg L^{-1}) in an anaerobic
479 fractured dolostone aquifer near an agrochemical facility (Parker et al., 2019). The persistence of
480 *S*-metolachlor in the laboratory aquifers thus indicates that long-term groundwater contamination
481 by *S*-metolachlor may occur, even under oxic conditions during stream-groundwater interactions.
482 Similarly, *metalaxyl*, *atrazine* and *terbutryn* proved persistent in both aquifers. *Metalaxyl*
483 attenuation was low to insignificant during all injection periods (SI, Section K). Mass recoveries
484 were 93 ± 4 % during both pulse injections (0−40 d and 90−40 d), while during the constant
485 injection period (40–90 d) metalaxyl concentrations followed those of atrazine and terbutryn (SI,
486 Section K). *Atrazine and terbutryn* also showed similar BTCs as the saline conservative tracer
487 (SI, Section K), indicating insignificant degradation or sorption over time. Atrazine is a highly
488 persistent substance and its accumulation in shallow groundwater has been proven even after
489 decades of its ban in 1992 in Germany (Vonberg et al., 2014). Moreover, the persistence of the
490 urban biocide terbutryn in both laboratory aquifers also suggests its accumulation in shallow
491 groundwater from entry pathways such as leaching of facades and urban stormwater infiltration
492 systems (Hensen et al., 2018).
493 Overall, the absence of significant biodegradation of metalaxyl, atrazine and terbutryn in
494 both laboratory aquifers agrees with observations from the stream water microcosms, where
495 biotransformation only occurred after 100 d (Figure 2). However, detection of TPs of metalaxyl
496 (demethylmetalaxyl), atrazine (deisopropylatrazine) and terbutryn (terbutryn sulfoxide, 2-
497 hydroxy-terbutryn and desethyl-terbutryn) suggested that the low attenuation (<10%) of these
498 micropollutants in the aquifers from 90 to 140 days was mainly associated with biodegradation
499 (SI, Section L).

3.3 C and N isotope fractionation of micropollutants

The insignificant stable isotope fractionation ($\Delta\delta^{13}C$ and $\Delta\delta^{15}N$ <2 ‰) for atrazine, terbutryn, metalaxyl and *S*-metolachlor confirmed their limited biodegradation in both aquifers (SI, Section K). However, $\delta^{13}C$ of caffeine featured a U-shaped trend during each injection period (Figure 3, middle panel), in particular during the second pulse injection (90−140 d). At low concentrations (<20 µg L^{-1}), i.e., at the front and tail of the BTCs, significant enrichment in ^{13}C of the non-degraded caffeine indicated the occurrence of caffeine biodegradation. In contrast, at peak concentrations, $\delta^{13}C$ values were similar to the source caffeine signature ($\delta^{13}C_0 = -31.4 \pm 0.1$ ‰) although significant mass removal occurred (Figure 3, upper panel).

A concentration dependence following Michaelis-Menten kinetics has been associated with the U-shaped of $\delta^{13}C$ values (Eckert et al., 2013; Schürner et al., 2016). This suggests that first-order kinetics may rather occur at low concentrations followed by a transition to zero-order kinetics at peak concentrations. The Michaelis-Menten type kinetics has thus been associated with an increase of the stable isotope fractionation at low pollutant concentrations, e.g., at a contaminant plume fringe (van Breukelen and Prommer, 2008). This agrees with the U-shaped $\delta^{13}C$ values observed for caffeine BTCs (Figure 3, middle panel). A similar stable isotope pattern was observed in a toluene pulse injection in a flow-through aquifer setup filled with natural sediment and groundwater (Eckert et al., 2013; Qiu et al., 2013). In the case of toluene in organic-rich sediment, the combination of both biodegradation and sorption resulted in U-shaped $\delta^{13}C$ trends slightly skewed toward the tail of the BTC (Qiu et al., 2013). This was interpreted as an effect of pollutant sorption to organic matter, which may be slightly stronger for pollutants with light isotopes than for those with heavy isotopes, leading to faster breakthrough of the heavy isotopologues (i.e., $^{12}K_d > {}^{13}K_d$ and $^{14}K_d > {}^{15}K_d$) (Kopinke et al., 2005). This would result

523 in an enrichment in ^{13}C at the contaminant front, while the BTC of ^{12}C isotopologues is expected
524 to cause a counteracting effect of the ^{13}C enriched signatures at the tail of the contaminant BTC
525 (Eckert et al., 2013).

526 Model simulations were performed to elucidate the U-shaped trend of $\delta^{13}C$ values
527 observed during caffeine biotransformation. Results from simulations of all injected periods are
528 presented in Section G of the SI. Overall, the simple RTM was able to capture the U-shaped
529 trend of $\delta^{13}C$ values. A good model fitting was observed for both caffeine BTC and $\delta^{13}C$ values,
530 particularly for the pulse-like injection periods (Figure 4 and SI, Section G). For the constant
531 injection period (40-90 days), however, concentrations and $\delta^{13}C$ values were difficult to predict
532 (SI, Section G). This could be explained by the scattered concentration data observed between
533 80-90 days, possibly due to clogging effects altering the flow paths, and the sensitivity towards
534 the biokinetic parameter for fitting the BTC fringes (Eckert et al., 2013). Nevertheless, similar
535 $\varepsilon_{c,bio}$ values were estimated in all the injection periods ranging from –0.32 to –0.40 ± 0.10 ‰ and
536 are close to the ε_c value reported for caffeine degradation in an oxic SWI microcosm (ε_c = –0.7 ±
537 0.1 ‰) (Droz et al., 2021). The computed $\varepsilon_{c,bio}$ values for caffeine biotransformation in the
538 laboratory aquifers may also be indicative of distinct competing degradation pathways (van
539 Breukelen, 2007) compared to the stream water microcosms, giving the wide range of bacteria
540 co-occurring in the laboratory aquifers (see below). Finally, the effect of sorption on the U-
541 shaped trend of $\delta^{13}C$ values was negligible (for all periods $\varepsilon_{c,sorb}$ < 0.06‰), confirming
542 insignificant caffeine sorption in the aquifers (Figures 3 and 4), in agreement with the absence of
543 significant shifts to higher retention times.

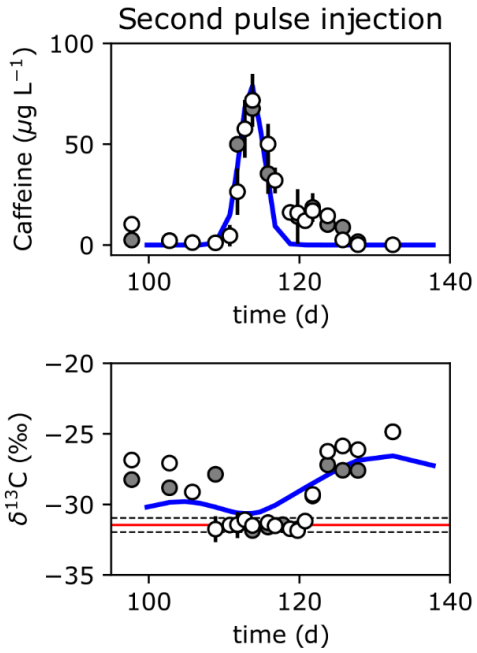

Figure 4. Simulated caffeine BTC (top) and carbon isotope signatures ($\delta^{13}C$; bottom) during the second pulse injection (93−140 d). Blue lines represent simulated reactive transport of caffeine. Grey and empty symbols represent datasets from both laboratory aquifers. Error bars correspond to the total analytical uncertainty accounting both accuracy and reproducibility of measurements (n=3). The red horizontal line (bottom) represents caffeine EA values of carbon (−31.46 ± 0.02‰) isotopes. Dashed horizontal lines (bottom) represent the total uncertainty of carbon ± 0.5‰ isotope analysis.

Overall, model simulations confirmed that the U-shaped $\delta^{13}C$ trend was associated with a concentration dependence upon caffeine biodegradation. This suggests that modeling Michaelis-Menten kinetics could realistically represent degradation behavior of micropollutants. The fitting of the caffeine BTC and $\delta^{13}C$ values was highly dependent on the biokinetic parameters, i.e., the r_{max} and K_m, resulting in significant stable isotope fractionation at the BTC fringes at low caffeine concentrations (Figure 4). A simple model formulation can thus result in good model predictions based on concentrations and stable isotopic data only. Nevertheless, Eckert et al.

(2013) pointed out that a trade-off between goodness of fit of both concentrations and stable isotopes should be considered, limiting a unique and reliable set of biokinetic parameters. Since biokinetic parameters are linked to the occurrence and evolution of bacterial degraders, an explicit formulation of the evolution of their biomass may ultimately improve model predictions. Moreover, modeling the reactive transport of micropollutant mixtures should also account for the inhibition of maximum degradation rates due to potential toxicity effects and competition among potential degraders. Further, the U-shaped trend of $\delta^{13}C$ values during micropollutant biodegradation in aquifers highlights the need for appropriate monitoring strategies to capture isotopic shifts in field scenarios. This would require an understanding of stream-groundwater flow interactions to predict micropollutants loadings in shallow aquifers (Hintze et al., 2020) and capture micropollutants BTC.

3.4 Gradual bacterial adaptations during transient micropollutants exposure

A gradual increase in bacterial diversity was observed in both aquifers over time and according to the transient exposure periods. NMDS ordination of the relative OTUs abundance showed that bacterial diversity mainly varied with the exposure periods (SI, Section M). A first shift in the bacterial diversity occurred from 0 to 38 days, following the acclimation period and the first pulse injection of micropollutants (i.e., acute exposure at 6 mg L^{-1}). This may be due to the pre-exposure of bacteria to micropollutants, possibly leading to a series of enzyme induction processes triggering pollutant biotransformation in the aquifers (Poursat et al., 2019b). This degradation potential within the aquifers was also demonstrated for caffeine degradation during the first injection period (Figure 2 and SI, Section L).

A second change in the bacterial diversity occurred from 90 to 140 d, following the constant and second pulse injection periods, respectively. This indicates the development of a

584 distinct bacterial community diversity following the chronic exposure at 600 µg L^{-1}, which may
585 coincide with a selective pressure of the micropollutant mixture for 21 consecutive days (SI,
586 Section M). Hence, a long-term exposure to the micropollutants may drive bacterial adaptation in
587 aquifers, possibly inducing changes at the community level or individual cells, e.g., by increasing
588 competitive strains (Kovárová-Kovar & Egli, 1998; Murínová & Dercová, 2014). Interestingly, a
589 slight shift of the bacterial diversity occurred at 220 d, while no micropollutant exposure
590 occurred from 140 to 220 d. This suggests the establishment of a well-adapted bacterial
591 community (SI, Section M), which was also observed in the sand cores at the end of the
592 experiments (SI, Section N). This idea is supported by the gradual increase in species richness
593 from 0 to 220 d, as emphasized by the increase in α-diversity (SI, Section M).

594 Accordingly, the bacterial community composition also varied over time. Differences
595 among the duplicate aquifers were observed in pore water samples, particularly within the
596 aquifers, possibly due to integrated pore water samples at different depth distances. However, the
597 trends in bacterial dynamics in both aquifers were consistent over time (Figure 5). Proteobacteria
598 dominated in pore water samples during all exposure periods (Figure 5). However, the change in
599 bacterial community composition (phylum level) after the first pulse injection (0−40 d) likely
600 corresponds to a first community response, which may be associated with the micropollutant
601 inflow in both aquifers. The abundance of Actinobacteria, Bacteroidetes and Elusimicrobia
602 increased to up to 25%, 8% and 45%, respectively, after the constant and the second pulse
603 injection periods (90 to 140 d) (Figure 5). At the end of the experiments (at 220 d),
604 Actinobacteria phylum remained as the second most abundant in pore water samples (up to
605 22%). This is in agreement with a previous study showing an increase in Actinobacteria and
606 associated genera in sediments of the HZ mimicked in river-simulating flumes (Posselt et al.,

2020). Although the bacterial diversity did not vary spatially over distance from inflow (SI, Section M), the bacterial community composition near the inflow (x=45 cm; Figure 5) differed from that at the outflow (x=160 cm). This is likely due to the vicinity of the source zone of micropollutants and thus higher exposure to micropollutants at the aquifer inflow (Figure 5). This was also observed for the attached bacteria retrieved from sand cores at the end of the experiments (220 d; SI, Section N), supporting the development of adapted bacterial communities even after the cease of transient micropollutant exposures.

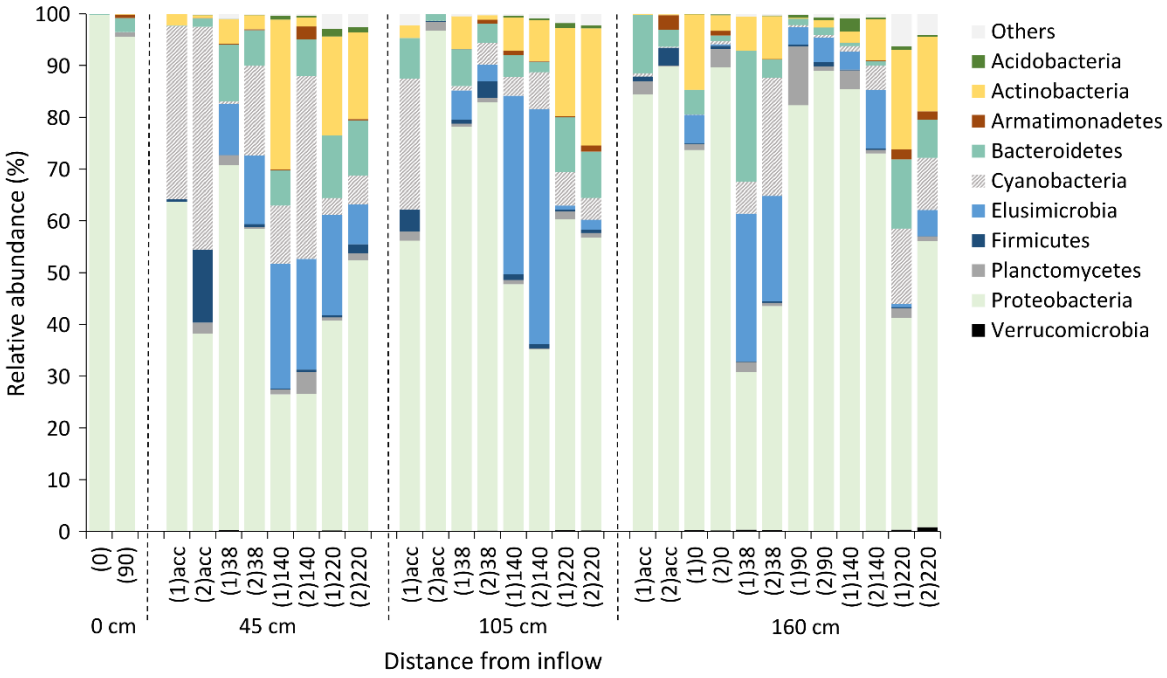

Figure 5. Relative abundance of bacterial phyla in pore water samples during transient exposures to the micropollutant mixture in the laboratory aquifers. Labels in brackets represent samples collected from the duplicate laboratory aquifers (1 and 2). Pore water samples were collected prior to the experiments (acc; acclimation period); after acclimation period (0 d), at the end of the first pulse injection (38 d), constant injection (90 d), and second injection periods (140 d). Samples were collected in the aquifer at 45 cm and 105 cm from the inflow, and from the outlet (x = 160 cm). 220 d correspond to the end of the experiment prior to core sand sampling.

623 The phylum Actinobacteria has been associated with pesticide biodegradation and
624 proposed for pollutant cleanup applications (Mawang et al., 2021). For instance, *Arthrobacter* sp.
625 and *Rhodococuss* sp. have been described for atrazine biodegradation in agricultural soils
626 (Sagarkar et al., 2014) and inoculated chemostats (Ehrl et al., 2019; Kundu et al., 2019).
627 Although atrazine biodegradation was not significant (<5%) in both aquifers, the increase in
628 Actinobacteria suggests a gradual increase of competent bacteria degraders in the aquifers. This
629 gradual increase in competent bacteria coincides with the lag-phase (up to 100 d) observed for
630 the degradation of most micropollutants in the stream water microcosm experiments (Figure 2).
631 Hence, bacterial tolerance and adaptation to long-term micropollutant exposure may be
632 established in both aquifers. Although caffeine degradation may be associated with
633 *Pseudomonas* sp. (Summers et al., 2015), *Pseudomonas* taxa accounted for <3% of the total
634 sequences (SI, Section O). This indicates a wide array of yet unexplored taxa potentially
635 involved in micropollutant degradation, notably for caffeine and metformin, urging for
636 fundamental studies on the identification of active micropollutant degraders and their metabolic
637 pathways.
638
639 **4. Conclusion**
640 The ubiquitous release of diverse micropollutant mixtures, from urban and/or agricultural
641 sources, into surface and groundwater has urged for improved environmental studies
642 representing more realistic field conditions. Current research issues in the field of micropollutant
643 transformation in polluted shallow aquifers include (i) how the contribution of degradative
644 processes can be evaluated, and (ii) what are the factors controlling micropollutant
645 biotransformation. Integrative studies such as ours, based on high resolution sampling from

laboratory aquifers mimicking stream water interactions with adjacent groundwater, may help to address these issues and enable more robust and long-term assessment of *in situ* transformation of micropollutants under transient exposure periods associated with seasonal applications and hydrological dynamics across stream-groundwater interfaces.

Specifically, our study highlighted that biotransformation of micropollutants as chemical mixtures largely varies, independently on the acute or chronic level of exposure to micropollutants. For instance, caffeine biotransformation, evaluated with carbon and nitrogen CSIA and the TPs formation, was observed during all micropollutants injection periods. In contrast, only moderate or negligible biotransformation of metformin, atrazine, terbutryn, *S*-metolachlor and metalaxyl occurred in the laboratory aquifers, indicating their persistence. CSIA of micropollutants can reinforce the evaluation of degradation or persistence of micropollutants in groundwater and identify 'hot and cold periods' of *in situ* biotransformation for assessing natural attenuation at the stream-groundwater interface. The integration of biomolecular markers such as 16S rRNA enabled to examine long-term acclimation and adaptation of bacterial communities and may be used as indicators of micropollutant biotransformation in groundwater. Taken together, our results highlight the relevance of laboratory aquifers fed with natural stream water and integrating DNA- and isotopic analyses to study and improve the assessment of emerging pollutants in shallow groundwater connected to streams.

Acknowledgments

This research was funded by the EC2CO-BIOHEFECT program (CNRS-INSU) through the 2D-DCM project and by the 80|Prime program (CNRS) through the project 3D-MICROPOL attributed to G.I. M.P.E. was supported by a fellowship of the Ecole Nationale du Génie de l'Eau

et de environment (ENGEES, France) and the doctoral school Earth and Environmental Sciences (ED 413) of University of Strasbourg. We are grateful to Benoît Guyot and Colin Fourtet for technical assistance in the laboratory, François Lehmann for help in mounting the laboratory aquifers and preliminary surveys, Emilie Muller for DNA data deposition and Jérémy Masbou for fruitful discussions. Elemental and isotopic analyses were performed at the Pacite platform of University of Strasbourg at ITES (Strasbourg, France).

Author Contributions

Maria Prieto-Espinoza: Investigation, Conceptualization, Methodology, Data curation, Visualization, Formal analysis, Writing - original draft, Writing - review & editing. Raphaël di Chiara: Investigation, Methodology, Writing - review & editing. Benjamin Belfort: Conceptualization, Methodology, Writing - review & editing. Sylvain Weill: Conceptualization, Writing - review & editing. Gwenaël Imfeld: Conceptualization, Formal analysis, Funding acquisition, Project administration, Resources, Supervision, Writing - review & editing.

Declaration of Competing Interests

The authors declare that they have no known competing financial interests or personal relationships that could have appeared to influence the work reported in this paper.

References

Alvarez-Zaldívar, P., Payraudeau, S., Meite, F., Masbou, J., & Imfeld, G., 2018. Pesticide degradation and export losses at the catchment scale: Insights from compound-specific isotope analysis (CSIA). Water Res., 139, 198–207. https://doi.org/10.1016/j.watres.2018.03.061

aus der Beek, T., Weber, F.-A., Bergmann, A., Hickmann, S., Ebert, I., Hein, A., & Küster, A., 2016. Pharmaceuticals in the environment – Global occurrences and perspectives. Environ. Toxicol. Chem., 35(4), 823–835. https://doi.org/10.1002/etc.3339

Baran, N., Surdyk, N., & Auterives, C., 2021. Pesticides in groundwater at a national scale (France): Impact of regulations, molecular properties, uses, hydrogeology and climatic conditions. Sci. Total Environ. 791, 148137. https://doi.org/10.1016/j.scitotenv.2021.148137

Barbosa, M. O., Moreira, N. F. F., Ribeiro, A. R., Pereira, M. F. R., & Silva, A. M. T., 2016. Occurrence and removal of organic micropollutants: an overview of the watch list of EU decision 2015/495. Water Res., 94, 257–279. https://doi.org/10.1016/j.watres.2016.02.047

Bauer, R. D., Rolle, M., Kürzinger, P., Grathwohl, P., Meckenstock, R. U., & Griebler, C., 2009. Two-dimensional flow-through microcosms – Versatile test systems to study biodegradation processes in porous aquifers. J. Hydrol., 369(3–4), 284–295. https://doi.org/10.1016/j.jhydrol.2009.02.037

Boulton, A. J., Datry, T., Kasahara, T., Mutz, M., & Stanford, J. A., 2010. Ecology and management of the hyporheic zone: Stream-groundwater interactions of running waters and their floodplains. J. North Am. Benthol. Soc., 29(1), 26–40. https://doi.org/10.1899/08-017.1

Bradley, P. M., Journey, C. A., Romanok, K. M., Breitmeyer, S. E., Button, D. T., Carlisle, D. M., Huffman B.J., Mahler B.J., Nowell L.H., Qi S.L., Smalling K.L., Waite R.I., & Van Metre, P.C., 2021. Multi-region assessment of chemical mixture exposures and predicted cumulative effects in USA wadeable urban/agriculture-gradient streams. Sci. Total Environ., 773, 145062, https://doi.org/10.1016/j.scitotenv.2021.145062

Bradley, P. M., Journey, C. A., Button, D. T., Carlisle, D. M., Clark, J. M., Mahler, B. J., Nakagaki, N., Qi, S. L., Waite, I. R., & VanMetre, P. C., 2016. Metformin and other

pharmaceuticals widespread in wadeable streams of the Southeastern United States. Environ. Sci. Technol. Lett., 3(6), 243–249. https://doi.org/10.1021/acs.estlett.6b00170

Buerge, I. J., Poiger, T., Müller, M. D., & Buser, H.-R., 2003. Enantioselective degradation of metalaxyl in soils: chiral preference changes with soil pH. Environ. Sci. Technol., 37(12), 2668–2674. https://doi.org/10.1021/es0202412

Cavalier, T. C., Lavy, T. L., & Mattice, J. D., 1991. Persistence of selected pesticides in ground-water samples. Groundwater, 29(2), 225–231. https://doi.org/10.1111/j.1745-6584.1991.tb00514.x

Chen, X., & Chen, X., 2003. Stream water infiltration, bank storage, and storage zone changes due to stream-stage fluctuations. J. Hydrol., 280(1–4), 246–264. https://doi.org/10.1016/S0022-1694(03)00232-4

Chow, R., Scheidegger, R., Doppler, T., Dietzel, A., Fenicia, F., & Stamm, C., 2020. A review of long-term pesticide monitoring studies to assess surface water quality trends. Water Res. X, 9, 100064. https://doi.org/10.1016/j.wroa.2020.100064

Conant, B., Robinson, C. E., Hinton, M. J., & Russell, H. A. J., 2019. A framework for conceptualizing groundwater-surface water interactions and identifying potential impacts on water quality, water quantity, and ecosystems. J. Hydrol., 574, 609–627. https://doi.org/10.1016/j.jhydrol.2019.04.050

Coplen, T. B., Brand, W. A., Gehre, M., Gröning, M., Meijer, H. A. J., Toman, B., & Verkouteren, R. M., 2006. New Guidelines for $\delta^{13}C$ Measurements. Anal. Chem., 78(7), 2439–2441. https://doi.org/10.1021/ac052027c

Dalmijn, J. A., Poursat, B. A. J., van Spanning, R. J. M., Brandt, B. W., de Voogt, P., & Parsons, J. R., 2021. Influence of short- and long-term exposure on the biodegradation capacity of activated sludge microbial communities in ready biodegradability tests. Environ. Sci. Water Res. Technol., 7(1), 107–121. https://doi.org/10.1039/D0EW00776E

Damalas, C. A., & Koutroubas, S. D., 2016. Farmers' exposure to pesticides: Toxicity types and ways of prevention. Toxics, 4(1), 1. https://doi.org/10.3390/toxics4010001

Dash, S. S., & Gummadi, S. N., 2007. Degradation kinetics of caffeine and related methylxanthines by induced cells of Pseudomonas sp. Curr. Microbiol, 55(1), 56–60. https://doi.org/10.1007/s00284-006-0588-2

748 Derx, J., Blaschke, A. P., & Blöschl, G., 2010. Three-dimensional flow patterns at the river–
749 aquifer interface – A case study at the Danube. Adv. Water Resour., 33(11), 1375–1387.
750 https://doi.org/10.1016/j.advwatres.2010.04.013
751 Drouin, G., Fahs, M., Droz, B., Younes, A., Imfeld, G., & Payraudeau, S., 2021. Pollutant
752 dissipation at the sediment- water interface: A robust discrete continuum numerical
753 model and recirculating laboratory experiments. Water Resour. Res., 57(3).
754 https://doi.org/10.1029/2020WR028932
755 Droz, B., 2020. Pesticides dissipation at the sediment-water interface: Insight from compound-
756 specific isotope analysis (CSIA) [Doctoral Thesis]. University of Strasbourg.
757 Droz, B., Drouin, G., Maurer, L., Villette, C., Payraudeau, S., & Imfeld, G., 2021. Phase transfer
758 and biodegradation of pesticides in water-sediment systems explored by compound-
759 specific isotope analysis and conceptual modeling. Environ. Sci. Technol., 55(8), 4720–
760 4728. https://doi.org/10.1021/acs.est.0c06283
761 Eckert, D., Qiu, S., Elsner, M., & Cirpka, O. A., 2013. Model complexity needed for quantitative
762 analysis of high-resolution isotope and concentration data from a toluene-pulse
763 experiment. Environ. Sci. Technol., 47(13), 6900–6907.
764 https://doi.org/10.1021/es304879d
765 Ehrl, B. N., Kundu, K., Gharasoo, M., Marozava, S., & Elsner, M., 2019. Rate-limiting mass
766 transfer in micropollutant degradation revealed by isotope fractionation in chemostat.
767 Environ. Sci. Technol., 53(3), 1197–1205. https://doi.org/10.1021/acs.est.8b05175
768 Elsayed, O. F., Maillard, E., Vuilleumier, S., Nijenhuis, I., Richnow, H. H., & Imfeld, G., 2014.
769 Using compound-specific isotope analysis to assess the degradation of chloroacetanilide
770 herbicides in lab-scale wetlands. Chemosphere, 99, 89–95.
771 https://doi.org/10.1016/j.chemosphere.2013.10.027
772 Elsner, M., 2010. Stable isotope fractionation to investigate natural transformation mechanisms
773 of organic contaminants: Principles, prospects and limitations. J. Environ. Monit., 12(11),
774 2005–2031. https://doi.org/10.1039/C0EM00277A
775 Elsner, M., & Imfeld, G., 2016. Compound-specific isotope analysis (CSIA) of micropollutants
776 in the environment—current developments and future challenges. Current Opinion in
777 Biotechnology, 41, 60-72, https://doi.org/10.1016/j.copbio.2016.04.014

778 Elsner, M., McKelvie, J., Lacrampe Couloume, G., & Sherwood Lollar, B., 2007. Insight into
779 methyl tert-butyl ether (MTBE) stable isotope fractionation from abiotic reference
780 experiments. Environ. Sci. Technol., 41(16), 5693–5700.
781 https://doi.org/10.1021/es070531o
782 Fenner, K., Canonica, S., Wackett, L. P., & Elsner, M., 2013. Evaluating pesticide degradation in
783 the environment: Blind spots and emerging opportunities. Science, 341(6147), 752–758.
784 https://doi.org/10.1126/science.1236281
785 Ghysels, G., Anibas, C., Awol, H., Tolche, A., Schneidewind, U., & Huysmans, M., 2021. The
786 significance of vertical and lateral groundwater-surface water exchange fluxes in
787 riverbeds and riverbanks: Comparing 1D analytical flux estimates with 3D groundwater
788 modelling. Water, 13(3), 306. https://doi.org/10.3390/w13030306
789 Hancock, P. J., 2002. Human impacts on the stream-groundwater exchange zone. J. Environ.
790 Manage., 29(6), 763–781. https://doi.org/10.1007/s00267-001-0064-5
791 Hellal, J., Joulian, C., Urien, C., Ferreira, S., Denonfoux, J., Hermon, L., Vuilleumier, S., &
792 Imfeld, G., 2021. Chlorinated ethene biodegradation and associated bacterial taxa in
793 multi-polluted groundwater: Insights from biomolecular markers and stable isotope
794 analysis. Sci. Total Environ., 763, 142950.
795 https://doi.org/10.1016/j.scitotenv.2020.142950
796 Hensen, B., Lange, J., Jackisch, N., Zieger, F., Olsson, O., & Kümmerer, K., 2018. Entry of
797 biocides and their transformation products into groundwater via urban stormwater
798 infiltration systems. Water Res., 144, 413–423.
799 https://doi.org/10.1016/j.watres.2018.07.046
800 Hildebrandt, A., Guillamón, M., Lacorte, S., Tauler, R., & Barceló, D., 2008. Impact of
801 pesticides used in agriculture and vineyards to surface and groundwater quality (North
802 Spain). Water Res., 42(13), 3315–3326. https://doi.org/10.1016/j.watres.2008.04.009
803 Hintze, S., Glauser, G., & Hunkeler, D., 2020. Influence of surface water–groundwater
804 interactions on the spatial distribution of pesticide metabolites in groundwater. Sci. Total
805 Environ., 733, 139109. https://doi.org/10.1016/j.scitotenv.2020.139109
806 Iker, B. C., Kambesis, P., Oehrle, S. A., Groves, C., & Barton, H. A., 2010. Microbial atrazine
807 breakdown in a karst groundwater system and its effect on ecosystem energetics. J.
808 Environ. Qual., 39(2), 509–518. https://doi.org/10.2134/jeq2009.0048

Jakobsen, R., Hinsby, K., Aamand, J., van der Keur, P., Kidmose, J., Purtschert, R., Jurgens, B., Sültenfuss, J., & Albers, C. N., 2019. History and sources of co-occurring pesticides in an abstraction well unraveled by age distributions of depth-specific groundwater samples. Environ. Sci. Technol., 54(1) 158–165. https://doi.org/10.1021/acs.est.9b03996

Kopinke, F.-D., Georgi, A., Voskamp, M., & Richnow, H. H., 2005. Carbon isotope fractionation of organic contaminants due to retardation on humic substances: Implications for natural attenuation studies in aquifers. Environ. Sci. Technol., 39(16), 6052–6062. https://doi.org/10.1021/es040096n

Koroša, A., Brenčič, M., & Mali, N., 2020. Estimating the transport parameters of propyphenazone, caffeine and carbamazepine by means of a tracer experiment in a coarse-gravel unsaturated zone. Water Res., 175, 115680. https://doi.org/10.1016/j.watres.2020.115680

Kovárová-Kovar, K., & Egli, T., 1998. Growth kinetics of suspended microbial cells: From single-substrate-controlled growth to mixed-substrate kinetics. Microbiol. Mol. Biol. Rev., 62(3), 646–666. https://doi.org/10.1128/MMBR.62.3.646-666.1998

Kundu, K., Marozava, S., Ehrl, B., Merl-Pham, J., Griebler, C., & Elsner, M., 2019. Defining lower limits of biodegradation: Atrazine degradation regulated by mass transfer and maintenance demand in Arthrobacter aurescens TC1. ISME J, 13(9), 2236–2251. https://doi.org/10.1038/s41396-019-0430-z

Lam, M. W., Young, C. J., Brain, R. A., Johnson, D. J., Hanson, M. A., Wilson, C. J., Richards, S. M., Solomon, K. R., & Mabury, S. A., 2004. Aquatic persistence of eight pharmaceuticals in a microcosm study. Environ. Toxicol. Chem., 23(6), 1431–1440. https://doi.org/10.1897/03-421

Lefrancq, M., Dijk, P. V., Jetten, V., Schwob, M., & Payraudeau, S., 2017. Improving runoff prediction using agronomical information in a cropped, loess covered catchment. Hydrol. Process., 31(6), 1408–1423. https://doi.org/10.1002/hyp.11115

Lesser, L. E., Mora, A., Moreau, C., Mahlknecht, J., Hernández-Antonio, A., Ramírez, A. I., & Barrios-Piña, H., 2018. Survey of 218 organic contaminants in groundwater derived from the world's largest untreated wastewater irrigation system: Mezquital Valley, Mexico. Chemosphere, 198, 510–521. https://doi.org/10.1016/j.chemosphere.2018.01.154

839 Lewandowski, J., Putschew, A., Schwesig, D., Neumann, C., & Radke, M., 2011. Fate of organic
840 micropollutants in the hyporheic zone of a eutrophic lowland stream: Results of a
841 preliminary field study. Sci. Total Environ., 409(10), 1824–1835.
842 https://doi.org/10.1016/j.scitotenv.2011.01.028
843 Loos, R., Locoro, G., Comero, S., Contini, S., Schwesig, D., Werres, F., Balsaa, P., Gans, O.,
844 Weiss, S., Blaha, L., Bolchi, M., & Gawlik, B. M., 2010. Pan-European survey on the
845 occurrence of selected polar organic persistent pollutants in ground water. Water Res.,
846 44(14), 4115–4126. https://doi.org/10.1016/j.watres.2010.05.032
847 Masoner, J. R., Kolpin, D. W., Cozzarelli, I. M., Barber, L. B., Burden, D. S., Foreman, W. T.,
848 Forshay, K. J., Furlong, E. T., Groves, J. F., Hladik, M. L., Hopton, M. E., Jaeschke, J.
849 B., Keefe, S. H., Krabbenhoft, D. P., Lowrance, R., Romanok, K. M., Rus, D. L., Selbig,
850 W. R., Williams, B. H., & Bradley, P. M., 2019. Urban stormwater: An overlooked
851 pathway of extensive mixed contaminants to surface and groundwaters in the United
852 States. Environ. Sci. Technol., 53(17), 10070–10081.
853 https://doi.org/10.1021/acs.est.9b02867
854 Mawang, C.-I., Azman, A.-S., Fuad, A.-S. M., & Ahamad, M., 2021. Actinobacteria: An eco-
855 friendly and promising technology for the bioaugmentation of contaminants. Biotechnol.
856 Rep., 32, e00679. https://doi.org/10.1016/j.btre.2021.e00679
857 Mechelke, J., Rust, D., Jaeger, A., & Hollender, J., 2020. Enantiomeric fractionation during
858 biotransformation of chiral pharmaceuticals in recirculating water-sediment test flumes.
859 Environ. Sci. Technol., 54(12), 7291–7301. https://doi.org/10.1021/acs.est.0c00767
860 Meckenstock, R. U., Elsner, M., Griebler, C., Lueders, T., Stumpp, C., Aamand, J., Agathos, S.
861 N., Albrechtsen, H.-J., Bastiaens, L., Bjerg, P. L., Boon, N., Dejonghe, W., Huang, W.
862 E., Schmidt, S. I., Smolders, E., Sørensen, S. R., Springael, D., & van Breukelen, B. M.,
863 2015. Biodegradation: Updating the concepts of control for microbial cleanup in
864 contaminated aquifers. Environ. Sci. Technol., 49(12), 7073–7081.
865 https://doi.org/10.1021/acs.est.5b00715
866 Murínová, S., & Dercová, K., 2014. Response mechanisms of bacterial degraders to
867 environmental contaminants on the level of cell walls and cytoplasmic membrane. Int. J.
868 Microbiol., 2014, 1–16. https://doi.org/10.1155/2014/873081

National Research Council., 2000. Natural attenuation for groundwater remediation. National Academies Press. https://doi.org/10.17226/9792

Nödler, K., Tsakiri, M., & Licha, T., 2014. The impact of different proportions of a treated effluent on the biotransformation of selected micro-contaminants in river water microcosms. Int. J. Environ. Res. Public Health, 11(10), 10390–10405. https://doi.org/10.3390/ijerph111010390

Ojeda, A. S., Phillips, E., & Lollar, B. S., 2020. Multi-element (C, H, Cl, Br) stable isotope fractionation as a tool to investigate transformation processes for halogenated hydrocarbons. Environ. Sci. Process. Impact, 22(3), 567-582.

Parker, B. L., Bairos, K., Maldaner, C. H., Chapman, S. W., Turner, C. M., Burns, L. S., Plett, J., Carter, R. and Cherry, J. A., 2019. Metolachlor dense non-aqueous phase liquid source conditions and plume attenuation in a dolostone water supply aquifer. Geological Society, London, Special Publications, 479(1), 207-236. https://doi.org/10.1144/SP479.9

Peter, K. T., Herzog, S., Tian, Z., Wu, C., McCray, J. E., Lynch, K., & Kolodziej, E. P., 2019. Evaluating emerging organic contaminant removal in an engineered hyporheic zone using high resolution mass spectrometry. Water Res., 150, 140–152. https://doi.org/10.1016/j.watres.2018.11.050

Posselt, M., Mechelke, J., Rutere, C., Coll, C., Jaeger, A., Raza, M., Meinikmann, K., Krause, S., Sobek, A., Lewandowski, J., Horn, M. A., Hollender, J., & Benskin, J. P., 2020. Bacterial diversity controls transformation of wastewater-derived organic contaminants in river-simulating flumes. Environ. Sci. Technol., 54(9), 5467–5479. https://doi.org/10.1021/acs.est.9b06928

Poursat, B. A. J., van Spanning, R. J. M., de Voogt, P., & Parsons, J. R., 2019a. Implications of microbial adaptation for the assessment of environmental persistence of chemicals. Crit. Rev. Environ. Sci. Technol., 49(23), 2220–2255. https://doi.org/10.1080/10643389.2019.1607687

Poursat, B. A. J., van Spanning, R. J. M., Braster, M., Helmus, R., de Voogt, P., & Parsons, J. R., 2019b. Biodegradation of metformin and its transformation product, guanylurea, by natural and exposed microbial communities. Ecotoxicol. Environ. Saf., 182, 109414. https://doi.org/10.1016/j.ecoenv.2019.109414

Prieto-Espinoza, M., Weill, S., Belfort, B., Muller, E. E. L., Masbou, J., Lehmann, F., Vuilleumier, S., & Imfeld, G., 2021. Water table fluctuations affect dichloromethane biodegradation in lab-scale aquifers contaminated with organohalides. Water Res., 203, 117530. https://doi.org/10.1016/j.watres.2021.117530

Qiu, S., Eckert, D., Cirpka, O. A., Huenniger, M., Knappett, P., Maloszewski, P., Meckenstock, R. U., Griebler, C., & Elsner, M., 2013. Direct experimental evidence of non-first order degradation kinetics and sorption-induced isotopic fractionation in a mesoscale aquifer: $^{13}C/\ ^{12}C$ analysis of a transient toluene pulse. Environ. Sci. Technol., 47(13), 6892–6899. https://doi.org/10.1021/es304877h

Reardon, K.F., Mosteller, D.C., Rogers, J.B., DuTeau, N.M., & Kim, et al., K., 2002. Biodegradation kinetics of aromatic hydrocarbon mixtures by pure and mixed bacterial cultures. EHP. 110, 1005-1011. https://doi.org/10.2307/3455676

Richardson, S. D., & Kimura, S. Y., 2016. Water analysis: Emerging contaminants and current issues. Anal. Chem., 88(1), 546–582. https://doi.org/10.1021/acs.analchem.5b04493

Sagarkar, S., Nousiainen, A., Shaligram, S., Björklöf, K., Lindström, K., Jørgensen, K. S., & Kapley, A., 2014. Soil mesocosm studies on atrazine bioremediation. Journal of Environ. Manage., 139, 208-216. https://doi.org/10.1016/j.jenvman.2014.02.016

Schaper, J. L., Posselt, M., McCallum, J. L., Banks, E. W., Hoehne, A., Meinikmann, K., Shanafield, M. A., Batelaan, O., & Lewandowski, J., 2018. Hyporheic exchange controls fate of trace organic compounds in an urban stream. Environ. Sci. Technol., 52(21), 12285–12294. https://doi.org/10.1021/acs.est.8b03117

Schürner, H. K. V., Maier, M. P., Eckert, D., Brejcha, R., Neumann, C.-C., Stumpp, C., Cirpka, O. A., & Elsner, M., 2016. Compound-specific stable isotope fractionation of pesticides and pharmaceuticals in a mesoscale aquifer model. Environ. Sci. Technol., 50(11), 5729–5739. https://doi.org/10.1021/acs.est.5b03828

Schwab, A. P., Splichal, P. A., & Banks, M. K., 2006. Persistence of atrazine and alachlor in ground water aquifers and soil. Wat. Air Soil Pollut., 171(1–4), 203–235. https://doi.org/10.1007/s11270-005-9037-2

Schwarzenbach, R. P., Egli, T., Hofstetter, T. B., von Gunten, U., & Wehrli, B., 2010. Global water pollution and human health. Annu. Rev. Environ. Resour., 35(1), 109–136. https://doi.org/10.1146/annurev-environ-100809-125342

930 Seiler, R. L., Zaugg, S. D., Thomas, J. M., & Howcroft, D. L., 1999. Caffeine and
931 pharmaceuticals as indicators of waste water contamination in wells. Groundwater, 37(3),
932 405–410. https://doi.org/10.1111/j.1745-6584.1999.tb01118.x
933 Straub, J. O., Caldwell, D. J., Davidson, T., D'Aco, V., Kappler, K., Robinson, P. F., Simon-
934 Hettich, B., & Tell, J., 2019. Environmental risk assessment of metformin and its
935 transformation product guanylurea. I. Environmental fate. Chemosphere, 216, 844–854.
936 https://doi.org/10.1016/j.chemosphere.2018.10.036
937 Summers, R. M., Mohanty, S. K., Gopishetty, S., & Subramanian, M., 2015. Genetic
938 characterization of caffeine degradation by bacteria and its potential applications. Microb.
939 Biotechnol., 8(3), 369–378. https://doi.org/10.1111/1751-7915.12262
940 Sun, F., Mellage, A., Gharasoo, M., Melsbach, A., Cao, X., Zimmermann, R., Griebler, C.,
941 Thullner, M., Cirpka, O. A., & Elsner, M., 2021a. Mass-transfer-limited biodegradation
942 at low concentrations - Evidence from reactive transport modeling of isotope profiles in a
943 bench-scale aquifer. Environ. Sci. Technol., 55(11), 7386-739.
944 https://doi.org/10.1021/acs.est.0c08566
945 Sun, F., Peters, J., Thullner, M., Cirpka, O. A., & Elsner, M., 2021b. Magnitude of diffusion- and
946 transverse dispersion-induced isotope fractionation of organic compounds in aqueous
947 systems. Environ. Sci. Technol., 55(8), 4772–4782.
948 https://doi.org/10.1021/acs.est.0c06741
949 Talja, K. M., Kaukonen, S., Kilpi-Koski, J., Malin, I., Kairesalo, T., Romantschuk, M.,
950 Tuominen, J., & Kontro, M. H., 2008. Atrazine and terbutryn degradation in deposits
951 from groundwater environment within the boreal region in Lahti, Finland. J. Agric. Food
952 Chem., 56(24), 11962–11968. https://doi.org/10.1021/jf802528a
953 Torabi, E., Wiegert, C., Guyot, B., Vuilleumier, S., & Imfeld, G., 2020. Dissipation of S-
954 metolachlor and butachlor in agricultural soils and responses of bacterial communities:
955 Insights from compound-specific isotope and biomolecular analyses. J. Environ, Sci., 92,
956 163-175. https://doi.org/10.1016/j.jes.2020.02.009
957 Van Breukelen, B. M., 2007. Extending the Rayleigh equation to allow competing isotope
958 fractionating pathways to improve quantification of biodegradation. Environ. Sci. Technol.,
959 41, 4004–4010. https://doi.org/10.1021/es0628452

Van Breukelen, B. M. V., & Prommer, H., 2008. Beyond the Rayleigh equation: Reactive transport modeling of isotope fractionation effects to improve quantification of biodegradation. Environ. Sci. Technol., 42(7), 2457–2463. https://doi.org/10.1021/es071981j

Vega, F. E., Emche, S., Shao, J., Simpkins, A., Summers, R. M., Mock, M. B., Ebert, D., Infante, F., Aoki, S., & Maul, J. E., 2021. Cultivation and genome sequencing of bacteria isolated from the coffee berry borer (*Hypothenemus hampei*), with emphasis on the role of caffeine degradation. Front. Microbiol., 12, 644768. https://doi.org/10.3389/fmicb.2021.644768

Vonberg, D., Vanderborght, J., Cremer, N., Pütz, T., Herbst, M., & Vereecken, H., 2014. 20 years of long-term atrazine monitoring in a shallow aquifer in western Germany. Water Res., 50, 294–306. https://doi.org/10.1016/j.watres.2013.10.032

Winter, T. C., Harvey, J. W., Franke, O. L., & Alley, W. M., 1998. Ground water and surface water a single resource [Circular]. U.S. Geological Survey.

Ye, Y., Chiogna, G., Cirpka, O., Grathwohl, P., & Rolle, M., 2015. Experimental investigation of compound-specific dilution of solute plumes in saturated porous media: 2-D vs. 3-D flow-through systems. J. Contam. Hydrol., 172, 33–47. https://doi.org/10.1016/j.jconhyd.2014.11.002

Yu, C. L., Louie, T. M., Summers, R., Kale, Y., Gopishetty, S., & Subramanian, M., 2009. Two distinct pathways for metabolism of theophylline and caffeine are coexpressed in Pseudomonas putida CBB5. J. Bacteriol., 191(14), 4624–4632. https://doi.org/10.1128/JB.00409-09

Zhang, Y., Wang, J., Yang, P., & Xie, S., 2017. Movement of lateral hyporheic flow between stream and groundwater. Sci. China Earth Sci., 60(11), 2033–2040. https://doi.org/10.1007/s11430-016-9103-9